Designed Synthesis of Solid State Structural Isomers from Modulated Reactants

Myungkeun Noh and David C. Johnson*

Department of Chemistry and Materials Science Institute, University of Oregon, Eugene, Oregon 97403

Received May 24, 1996[⊗]

Abstract: A series of new, kinetically stable, crystalline superlattice compounds containing integral number of intergrown dichalcogenide layers were prepared through controlled crystallization of Ti/Se/Nb/Se superlattice reactants with designed compositional modulation. Discussed in this paper is a family of structural isomers with the overall stoichiometry of $NbTiSe_4$. Specifically, the members of this series containing 1/1, 2/2, 3/3, 4/4, 6/6, 8/8, 9/9, 12/12, and 15/15 $TiSe_2/NbSe_2$ units as the unit cell of the superlattice were prepared as polycrystalline thin films oriented with the dichalcogenide layers perpendicular to the substrate surface. Low-angle diffraction data collected as a function of time and temperature reveal that the initial layered reactant contracts in the *c*-axis direction and that the interfaces become smoother during initial interdiffusion. Theta−theta scans show a gradual decrease of the (00*l*) diffraction line widths of the growing compound as a function of annealing time and temperature indicating an increase in the *c*-axis domain size. High-angle rocking curve diffraction data show increasing *c*-axis orientation, suggesting $TiSe_2/NbSe_2$ crystal growth perpendicular to the substrate surface upon low-temperature annealing. The end products of this synthetic approach are high quality *c*-axis-oriented $TiSe_2/NbSe_2$ crystalline superlattices with designed structure resulting from relatively low-temperature annealing at 500 °C. A working model for the formation of crystalline superlattices from the modulated reactants is presented which is consistent with the data.

Introduction

Synthetic molecular chemistry is based on the use of a series of kinetically controlled reactions to build the structure of the desired product molecule. Through studies of reaction rates and rate laws, reaction mechanisms have been developed which give a detailed molecular-level picture of how these reactions take place. This detailed understanding of the reaction mechanisms permits molecular chemists to carefully design and build reagents, and reactants to achieve a desired kinetic product by adjusting the relative kinetics of various reaction pathways. The development of this understanding has permitted chemists to prepare complicated natural products such as brevetoxin and palytoxin via rational synthetic strategies.

In significant contrast to synthetic molecular chemistry, the ability to control reaction kinetics in the solid state and to control the structure of the resulting product compounds is much less developed. The rate-limiting step in traditional solid state reactions is typically solid state diffusion. While solid state diffusion on long-length scales is understood, very little is known concerning the initial intermixing of solid state reactants and even less is understood regarding the molecular rearrangements required to nucleate the subsequent crystalline product. High reaction temperatures and long reaction times are usually used to overcome slow solid state diffusion rates and mix the reactants, leading to the thermodynamically most stable products.[1] Consequently, much less emphasis has been directed at developing methods to control reaction kinetics in the solid state. Indeed, the synthesis of novel solid state compounds is often stated to be as much an art as a science.[2]

Recently, the area of nanostructured materials has attracted intense interest directed at both fundamental issues and promising applications from both the molecular and solid state chemistry communities.[3] This interest derives in part from the recognition that dramatic changes in physical properties and chemical reactivity occur in systems confined to nanometer dimensions or modulated on nanometer length scales. The ability to produce nanostructured materials has already led to many advances in technology such as higher device speeds,[4] solid state lasers, and "band gap engineering" of materials[5] and also to fundamentally new physical phenomena such as the quantized Hall effect[6] and the fractional quantized Hall effect.[7] The preparation of these nanostructured materials, especially with sufficient crystalline order for structure determination, presents new synthetic challenges for both molecular and solid state chemists.

This paper describes the kinetic trapping of desired heterostructured products from the solid state reaction of designed superlattice reactants. In essence, this approach parallels that of molecular chemists in the development of a working model for the reaction mechanism which is subsequently used to aid design of reactants which will react to form desired kinetic products. In the work described herein, instead of molecules, we prepare interwoven layers of the elements within a superlattice reactant. Subsequent annealing at low temperatures results in interfacial nucleation and growth of the constituent heterostructure compounds which kinetically traps the desired superlattice structure. This approach may permit the preparation of heterostructures, such as those containing ternary compounds, which would be difficult to prepare using alternative approaches. It also is capable of quickly preparing significant amounts of product with control of the number of unit cells of each of the components making up the desired nanostructure. This paper

[⊗] Abstract published in *Advance ACS Abstracts,* September 1, 1996.

(1) Corbett, J. D. *Synthesis of Solid-State Materials*; Corbett, J. D., Ed.; Clarendon Press: Oxford, 1987; pp 1−38.

(2) DiSalvo, F. J. *Science* **1990**, *247*, 649−655.

(3) Ozin, G. A. *Adv. Mater.* **1992**, *4*, 612−648.

(4) Sano, N.; Kato, H.; Chiko, S. *Solid State Commun.* **1984**, *49*, 123.

(5) Capasso, F. *Physica* **1985**, *129B*, 92.

(6) Klitzing, K. v.; Dorda, G.; Pepper, M. *Phys. Rev. Lett.* **1980**, *45*, 494.

(7) Tsui, D. C.; Stormer, H. L.; Gossard, A. C. *Phys. Rev. Lett.* **1982**, *48*, 1559.

S0002-7863(96)01765-9 CCC: $12.00

Table 1. Intended Layer Thicknesses and Experimentally Determined Repeating Units for Samples Prepared as Part of This Study[a]

sample	intended Nb thickness (Å)	intended Se thickness (Å)	intended Ti thickness (Å)	intended Se thickness (Å)	measd repeat (as-deposited) (Å)	unit cell of superlattice product (Å)	calcd unit cell of superlattice (Å)
$[TiSe_2]_1[NbSe_2]_1$	1 × 1.31	1 × 5.46	1 × 1.36	1 × 5.17	12.72(10)	12.32(2)	12.43
$[TiSe_2]_2[NbSe_2]_2$	1 × 2.62	1 × 10.93	1 × 2.71	1 × 10.35	25.03(30)	24.83(21)	24.86
$[TiSe_2]_3[NbSe_2]_3$	1 × 3.93	1 × 16.39	1 × 4.07	1 × 15.52	38.35(30)	37.26(19)	37.29
$[TiSe_2]_4[NbSe_2]_4$	2 × 2.62	2 × 10.93	2 × 2.71	2 × 10.35	52.1(20)	48.4(11)	49.72
$[TiSe_2]_6[NbSe_2]_6$	2 × 3.93	2 × 16.39	2 × 4.07	2 × 2.62	77.2(20)	74.2(11)	74.6
$[TiSe_2]_8[NbSe_2]_8$	4 × 2.62	4 × 10.93	4 × 2.71	4 × 10.35	100.0(25)	99.0(15)	99.4
$[TiSe_2]_{12}[NbSe_2]_{12}$	4 × 3.93	4 × 16.39	4 × 4.07	4 × 15.52	154.6(30)	148.1(17)	149.2
$[TiSe_2]_{15}[NbSe_2]_{15}$	5 × 3.93	5 × 16.39	5 × 4.07	5 × 15.52	188.6(40)	185.6(28)	186.5

[a] For the intended elemental layer thicknesses, the first number is the number of times a layer was deposited. For example, in sample $[NbSe_2]_4[TiSe_2]_4$, the repeating pattern in the as-deposited sample was Ti/Se/Ti/Se/Nb/Se/Nb/Se with the thicknesses indicated. The calculated unit cell of the superlattice is based on the lattice parameters of the binary constituents. The measured unit cell of the superlattice is calculated using the high-angle 00*l* diffraction peaks on the basis of a least squares fitting procedure.

presents diffraction data used to support a reaction mechanism and the results of using this reaction mechanism to prepare a series of $NbTiSe_4$ structural isomers with designed superstructure.

Experimental Section

Synthesis of Samples. Samples were made in a custom-built ultrahigh vacuum chamber with independently controlled sources. Niobium and titanium were deposited at 0.5 Å/s by an electron beam gun that was controlled via a Leybold−Inficon XTC quartz crystal thickness monitor. Selenium was deposited using a Knudsen cell maintained at a constant temperature chosen to maintain a selenium deposition rate of approximately 1.0 Å/s by an Omega CN-9000 temperature−controller, and the rate of selenium deposition was monitored on a quartz crystal thickness monitor. Above each of the sources are computer-controlled shutters to allow precise control of elemental layer thicknesses.[8] The samples were deposited simultaneously on silicon substrates polished to ±3 Å root mean square (rms) for X-ray studies and on silicon wafers coated with poly(methylmethacrylate) for examining the evolution of the samples free of the substrate.

Grazing Angle and High-Angle X-ray Diffraction. X-ray data was collected on a Scintag 2000 $\theta-\theta$ diffractometer which has been modified to allow the sample height to be reproducibly adjusted by 0.0002 in. Alignment of the diffractometer was confirmed by checking that the rocking curve maxima due to specular reflection at several angles occurred when the incident and exit angles were equal. Grazing angle X-ray diffraction data were used to confirm the layered structure of the evolving superlattices and analyzed to determine the layer spacing. High-angle diffraction data were used to follow the evolution of crystalline order in the superlattices as a function of annealing temperature and time. The annealing of the samples was done in a drybox with a nitrogen atmosphere with less than 0.5 ppm oxygen.

Thermogravimetric Analysis (TGA). Thermogravimetric analysis was used to determine the actual stoichiometry of the calibration samples containing identical layer thicknesses of the Nb and Se (or Ti and Se) used in the initial ternary superlattice reactants. These samples were heated to 850 °C in flowing air and then held at this temperature for 2 h. The weight change recorded is the difference between mass loss due to the evaporation of excess Se and the weight gain resulting from the oxidation of the niobium forming Nb_2O_5 or titanium to TiO_2, as confirmed by X-ray diffraction.

Differential Scanning Calorimetry (DSC). The heat evolved by diffusion and growth was measured using a Du Pont TA9000 DSC module. Approximately 1 mg of sample free of the substrate was used in this experiment. The sample was heated to 550 °C at a rate of 10 °C/min under flowing nitrogen. This obtained the irreversible changes that occurred during the initial heating. The sample was cooled and reheated to 550 °C two additional times to obtain base lines of the reversible changes in the sample and the cell background. The net heat absorbed or released from the multilayer samples was obtained from the difference between the first and the subsequent runs.

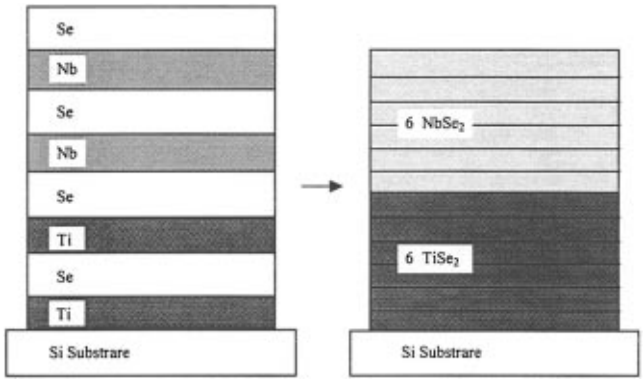

Figure 1. A schematic of the initial structure of the superlattice reactants used to prepare the $NbTiSe_4$ structural isomers.

Results and Discussion

A series of superlattice reactants with the overall structure shown in Figure 1 were prepared with varying thicknesses and number of niobium and titanium layers, as summarized in Table 1. Through calibration samples, the composition of each niobium−selenium and titanium−selenium block was adjusted to be that of the desired dichalcogenide compounds and the total amount of each component was chosen to be integral multiples of the known crystallographic unit cells, so there would be no elemental reactants left in the superlattice after extended annealing. On the basis of previous results,[9] low-temperature annealing was expected to result in the respective dichalcogenide products nucleating and growing along the reacting metal−selenium interfaces resulting in the dichalcogenide heterostructure as the kinetically trapped product, provided that alloying of the metals does not occur at the temperatures required to crystallize the structure. We expected that slow solid state diffusion rates would delay interdiffusion of the niobium and titanium through the intervening selenium layers, inhibiting the nucleation of the alloy or a ternary product.

We attempted to test our proposed model for superlattice formation, interfacial nucleation, and oriented crystal growth by examining the evolution of a superlattice reactant designed to form a crystalline superlattice with three $NbSe_2$ layers and three $TiSe_2$ layers in the unit cell as a function of annealing time and temperature. Figure 2 contains the evolution of the low-angle diffraction data as the sample is consecutively annealed for 8 h at each of the indicated temperatures. The Bragg diffraction maxima in the low-angle diffraction data

(8) Fister, L.; Li, X. M.; Novet, T.; McConnell, J.; Johnson, D. C. *J. Vac. Sci. Technol., A* **1993**, *11*, 3014−3019.

(9) Noh, M.; Thiel, J.; Johnson, D. C. *Science* **1995**, *270*, 1181−1184.

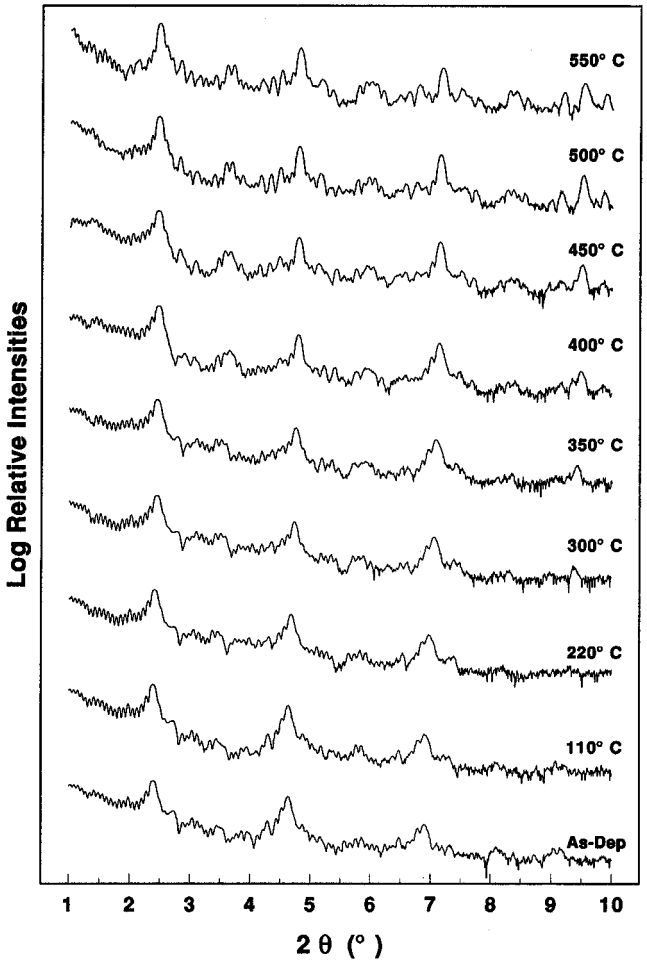

Figure 2. Low-angle diffraction data collected on a superlattice reactant in which elemental layers were deposited of appropriate thickness to yield three $TiSe_2$ layers and three $NbSe_2$ layers in the unit cell as a function of annealing temperature. The sample was annealed for 8 h at each of the indicated temperatures.

confirms the compositionally modulated nature of the as-deposited sample and clearly indicates that the sample remains compositionally modulated throughout the temperature range investigated. Significantly, there is little change in the intensity of the low-order superlattice diffraction maxima during the low-temperature annealing, indicative of little interdiffusion of the metal cations.[10] Upon annealing, there is also an initial increase in the intensity, regularity, and persistence with increasing angle of the subsidiary maxima, which result from a combination of incomplete destructive interference from the layers and front surface−back surface interference.[11] These changes in the subsidiary maxima all indicate that the sample becomes smoother during the initial interdiffusion reaction. Further evidence for the smoothing of the layers comes from rocking angle measurements on the low-angle diffraction maxima. As shown in Figure 3, the low-angle rocking curves consist of a sharp specular component on a broad nonspecular background. The intensity of the nonspecular scattering depends only on the magnitude of the rms roughness of the interfaces.[12] In Figure 4, the decrease in the amount of diffuse scattering on annealing

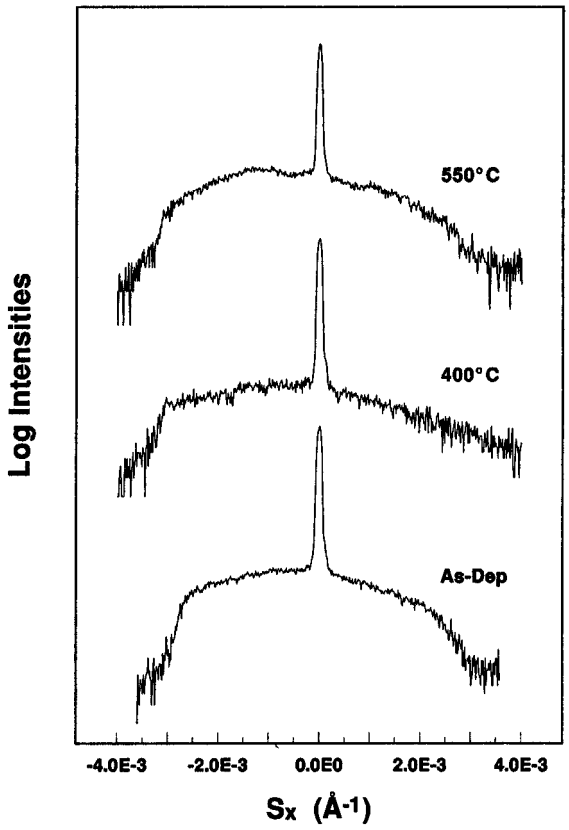

Figure 3. The low-angle rocking curve of the 002 Bragg diffraction maxima of the developing $[NbSe_2]_3[TiSe_2]_3$ superlattice, as a function of annealing temperature. The intensity of the broad nonspecular scattering depends only on the magnitude of the roughness of the interfaces.

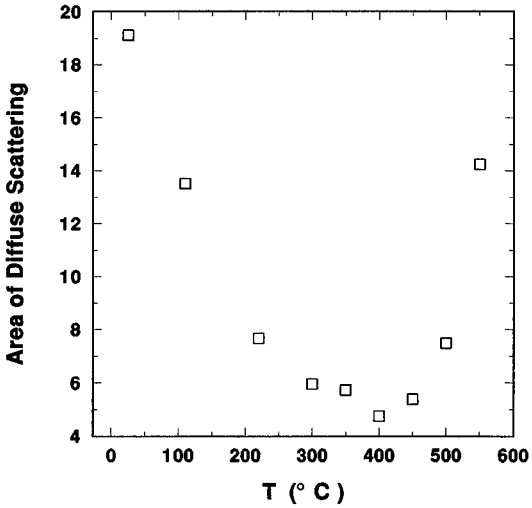

Figure 4. The change in the amount of diffuse scattering, measured using the integrated area of the nonspecular scattering around the 002 Bragg diffraction maxima, as a function of annealing temperature.

the sample at low temperatures, measured by the integrated area of the nonspecular scattering, is consistent with a decrease in the roughness of the interfaces. This smoothing is probably related to the elimination of voids in the structure, since the sample contracts by 3% during annealing.

High-angle diffraction data was also collected on the 3/3 superlattice during annealing, as shown in Figure 5. These diffraction patterns show the continuous evolution of the high-angle 00*l* Bragg diffraction peaks as the dichalcogenide nuclei grow. Differential scanning calorimetry data collected on samples in this series show the continual evolution of heat with

(10) Novet, T.; McConnell, J. M.; Johnson, D. C. *Chem. Mater*. **1992**, *4*, 473−478.

(11) Novet, T.; Johnson, D. C.; Fister, L. In *Interfaces, Interfacial Reactions, and Superlattice Reactants*; Novet, T., Johnson, D. C., Fister, L., Eds.; American Chemical Society: Washington, DC, 1995; Vol. 245, pp 425−470.

(12) Savage, D. E.; Kleiner, J.; Schimke, N.; Phang, Y.-H.; Jankowski, T.; Jacobs, J.; Kariotis, R.; Lagally, M. G. *J. Appl. Phys*. **1991**, *69*, 1411−1424.

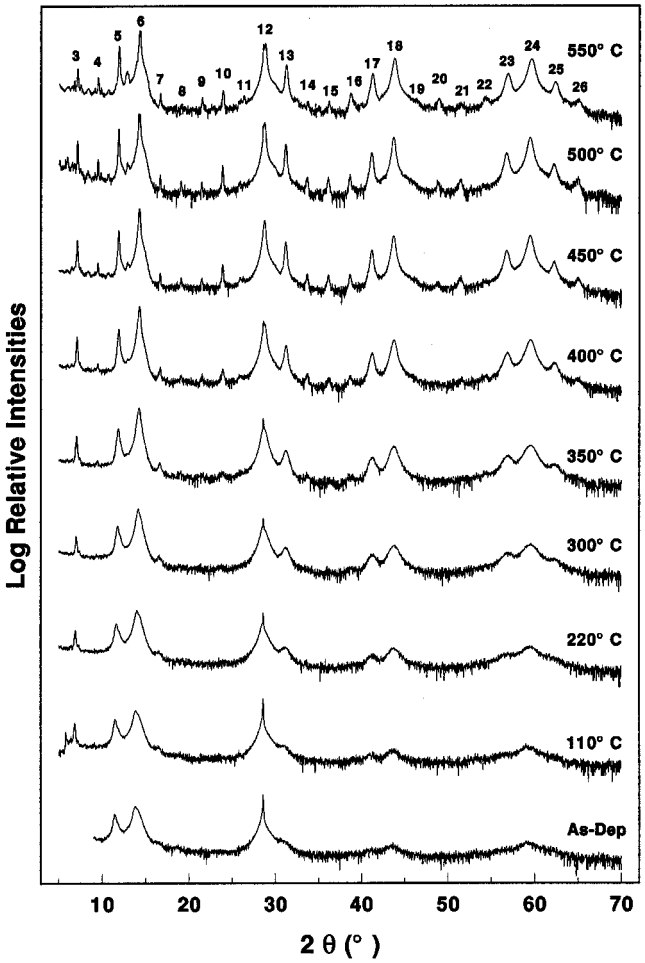

Figure 5. High-angle diffraction data collected on the developing $[TiSe_2]_3[NbSe_2]_3$ superlattice as a function of annealing temperature.

increasing temperature indicative of the continued growth of the dichalcogenide nuclei. The broad diffraction maxima evident at high angles in the diffraction pattern of the as-deposited sample indicate that nucleation of the dichalcogenide layers occurs during deposition. Annealing below 300 °C increases the intensity of the diffraction maxima without decreasing the line width, indicating that the amount of material crystallized is increasing without increasing the domain size perpendicular to the layers. This suggests that at low annealing temperatures, the crystallites grow along the interfacial planes rather than perpendicular to them. Crystal growth perpendicular to the interfacial planes during annealing is clearly evident in data collected after annealing above 350 °C through the sharpening of the diffraction pattern as a function of annealing time and temperature. As shown in Figure 6, the line width of the high-angle diffraction maxima decreases with continued annealing. When the annealing is continued at the highest temperature, there is a decrease in the intensity of the high-angle diffraction maxima due to the beginning of mixing of the niobium and titanium cations in the dichalcogenide layers.

Rocking curve diffraction scans taken as a function of annealing temperature of the developing high-angle diffraction maxima show a narrowing with increasing annealing time and temperature, with the half widths of the 006 Bragg diffraction maxima decreasing from 1.41 to 0.07°, as shown in Figure 7. While the peak widths of the Bragg diffraction maxima are related to the size of the crystallites, the rocking curve widths determine the degree of preferred orientation of the crystallites. The observed narrowing with annealing indicates that the degree of alignment of the superlattice with the substrate gradually

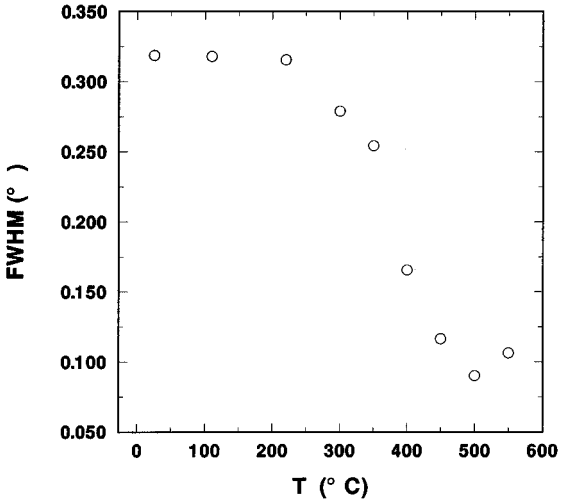

Figure 6. The change in the line width of the 005 high-angle diffraction maxima as a function of annealing temperature.

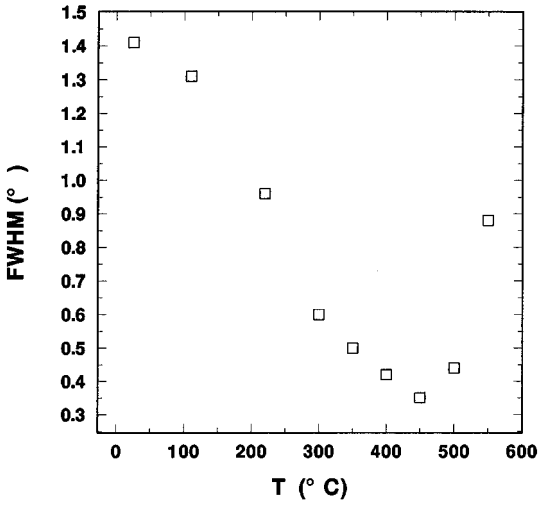

Figure 7. The change in the line width of the high-angle rocking curve of the 006 Bragg diffraction maxima of the developing $[TiSe_2]_3[NbSe_2]_3$ superlattice as a function of annealing temperature.

increases as the sample evolves into the desired, kinetically trapped crystalline superlattice with the 00*l* diffraction planes aligned parallel with initial interfaces present in the superlattice reactant.

The diffraction data discussed above is consistent with low-temperature interfacial nucleation of the binary components followed by grain growth. The narrowing of the rocking curves upon annealing suggest preferential grain growth of crystals along the interfaces which are parallel to the substrate. This preferential growth occurs because only the interface regions contain the correct atomic ratios of the elements to sustain grain growth without long-range diffusion. This low-temperature grain growth is important, since the "pancake-like" domains which form perhaps act as diffusion barriers inhibiting subsequent interdiffusion of the transition metals. These data suggest that the optimum growth conditions for obtaining crystalline superlattices begin with a low-temperature annealing to nucleate and grow the desired component compounds at and along the interfaces. Subsequent higher temperature annealing leads to grain growth and eliminates defects and misoriented crystallites. The time required for this annealing will depend upon diffusion rates; however, the maximum temperature of this anneal is limited by the energy required to exchange and interdiffuse the metals in the respective dichalcogenides, which occurs at approximately 650 °C in this system.

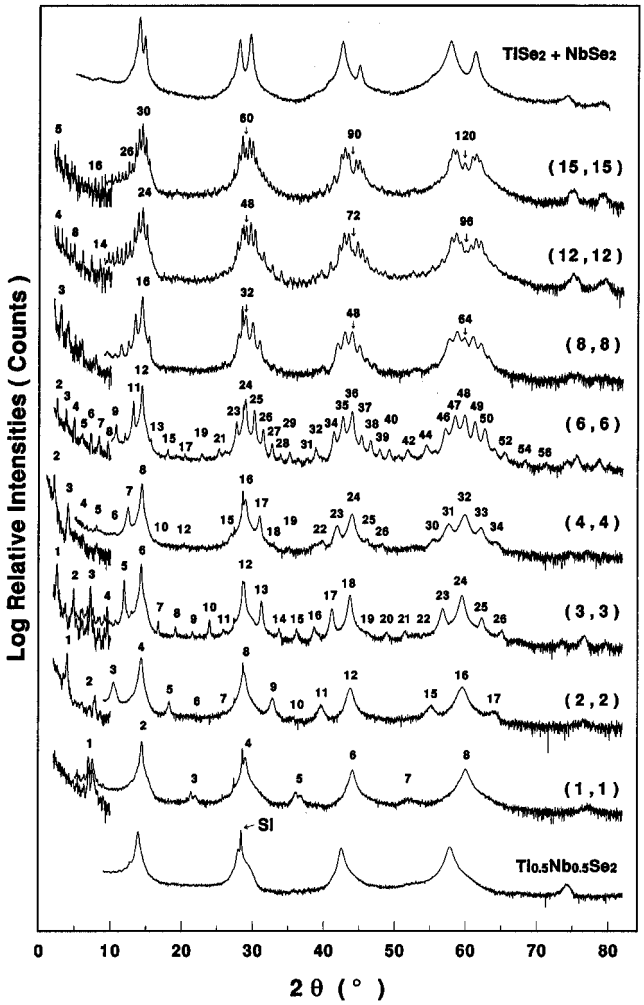

Figure 8. Diffraction data collected on series of structural isomers of composition $TiNbSe_4$ containing equal numbers of crystallographic layers of the respective dichalcogenide compounds in the unit cell. The diffraction patterns of the members of this series containing the homogeneous alloy (bottom diffraction pattern), 1/1, 2/2, 3/3, 4/4, 6/6, 8/8, 9/9, 12/12, and 15/15 $TiSe_2/NbSe_2$ units as the unit cell of the superlattice, and a mixture of the binary compounds (top diffraction pattern) are shown as an offset for clarity.

The superlattice reactants summarized in Table 1 were annealed for similar temperatures and times as the $[TiSe_2]_3$-$[NbSe_2]_3$ discussed in detail above. The reactants evolved into crystalline superlattices containing many well-resolved diffraction maxima, as shown in Figure 8. All of the diffraction maxima in the diffraction patterns can be indexed as 00*l* diffraction maxima resulting in *c*-axis lattice parameters consistent with the desired number *N*, of $NbSe_2$ layers and $TiSe_2$ layers in the repeating unit of the superlattice sample, as summarized in Figure 9. The diffraction patterns are qualitatively what is expected for the intended structures consisting of the convolution of the supercell diffraction on top of that expected for the dichalcogenides. For the $[TiSe_2]_6[NbSe_2]_6$ sample, we searched for and found the 10*l* diffraction intensity in reflection mode on a single-crystal diffractometer. The diffraction signal consisted of a ring of intensity, indicating that we have well-formed dichalcogenide layers but that they are not uniformly oriented in the *ab*-plane due to multiple domains. This is consistent with interfacial nucleation of the layers, whereas epitaxial growth would result in a preferred orientation of the *ab*-plane relative to the substrate. As order in the plane perpendicular to the *c*-axis develops, the ring of intensity should evolve into a hexagonal pattern of intensity. The high quality

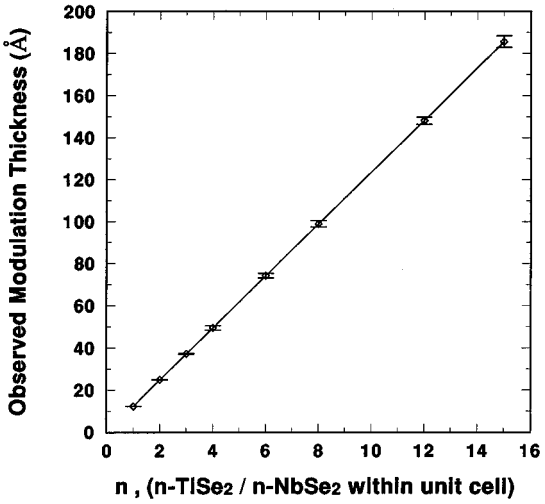

Figure 9. A plot of the refined *c*-axis lattice parameters versus the desired number of repeating units *N*. The linear relationship between these parameters highlights the ability of this approach to design the structure of the desired final product through control of the initial reactant.

of the 00*l* diffraction patterns, however, highlights the well-formed structure which develops along the *c*-axis as the superlattice structure is kinetically trapped.

The quality of the 00*l* diffraction data shown in Figure 8 permitted us to gain further insight into the structure of our superlattices by considering the structure as being composed as a single large unit cell consisting of multiple units similar to those of the parent structures. The refined structure of the $[TiSe_2]_6[NbSe_2]_6$ crystalline superlattice, reported previously,[9] contains the expected structural components based upon the structure of the initial multilayer reactant. As designed, the structure contains six layers of titanium diselenide and six layers of niobium diselenide with interlayer distances bracketed by those found in polytypes of the pure dichalcogenides. At the boundary between the niobium and titanium dichalcogenides, we found one layer with significant mixed metal population. Since titanium is always octahedral in the dichalcogenides but niobium can be either octahedral or trigonal prismatic coordinated, we find a more abrupt boundary at the niobium-mixed metal boundary than at the titanium−mixed metal boundary. The van der Waals gaps in both the niobium and titanium dichalcogenide layers are comparable to those found in the pure dichalcogenides, while the gap between the titanium and niobium dichalcogenides is slightly larger. This is perhaps a result of the *a*-axis mismatch between the dichalcogenides. Use of this structure as a model in each of the diffraction patterns shown in Figure 8 results in qualitative agreement with the intensities of the observed diffraction maxima. Determining the average structure in the layering direction from the resulting diffraction patterns using Rietveld refinement has proven to be problematic. The major difficulty is that the difference in intensity between the large diffraction maxima, resulting from constructive interference of the diffraction from the respective layers, and the small diffraction maxima, resulting from the incomplete destructive interference of diffraction from the respective layers due to the compositional modulation in the superstructure, is greater than 5 orders of magnitude. Errors in fitting the tails of the larger peaks due to errors in the chosen profiles significantly change the fitted intensity of the small peaks. These errors dramatically effect the relative occupancies of the niobium and titanium in the metal site of the dichalcogenide layers. These occupancies determine the profile of the compositional modulation through the interface regions.

Four probe electrical conductivity measurements parallel to the superlattice modulation were made on the $[NbSe_2]_3[TiSe_2]_3$, $[NbSe_2]_6[TiSe_2]_6$, $[NbSe_2]_9[TiSe_2]_9$, $[NbSe_2]_{12}[TiSe_2]_{12}$, and $[NbSe_2]_{15}[TiSe_2]_{15}$ superlattices. The conductivity data for all of the samples were similar, displaying metallic behavior as expected from the properties of the components. All of the samples, however, showed a small increase in resistivity at low temperatures, presumably due to intergrain contact resistances. While both the $[TiSe_2]_3[NbSe_2]_3$ and $[TiSe_2]_6[NbSe_2]_6$ samples displayed normal conducting behavior down to 1.2 K, superconducting critical temperatures of 2.8 and 3.2 K were observed for the $[TiSe_2]_9[NbSe_2]_9$ and $[TiSe_2]_{12}[NbSe_2]_{12}$ samples, respectively. Surprisingly, the $[TiSe_2]_{15}[NbSe_2]_{15}$ sample was not found to superconduct above 1.2 K. The lack of superconductivity in the two shortest repeat length samples might result from the $NbSe_2$ layer thicknesses being below the superconducting coherence length for $NbSe_2$ (27 Å in the *cis*-axis direction).[13] The behavior of the thickest sample, however, cannot be explained in this manner. Additional samples are being prepared to confirm these conductivity measurements and further probe the dependence of electrical properties on superlattice structure.

The results presented highlight the potential to synthesize new "designed" layer structures of many kinds using superlattice reactants. This in turn implies the possible design of physical and chemical properties. Understanding the development of physical properties as a function of length scale requires understanding charge transfer and bonding changes at the interfaces, subjects which are presently not very well understood. This synthetic advance sets the stage for unexpected atomic-bonding and mechanical and electrical properties which can be systematically examined as a function of heterostructure length scales. Other phenomena, such as phase transformations and interface-related processes in thin-film and layered alloys, may also be profoundly different in these heterostructured materials from what is now well-known in the bulk alloy or composite systems.

Summary

The ability to prepare intergrowth compounds from superlattice reactants as described herein permits the tailoring of physical properties as a function of compositional layer thicknesses and native properties of the parent compounds as done previously for compound semiconductors. As the length scale of the compositional modulation decreases, a transition from composite behavior to that of a new compound should occur with the length scale of the transition, depending upon the property being monitored. Kinetic trapping from superlattice reactants potentially increases the variety of compounds which can be intergrown, since this approach is only limited by the ability to prepare the reactants with suitable compositions and finding annealing conditions which permit growth of crystallites without significant interdiffusion of the multilayer components. Understanding the reaction mechanism of this synthetic pathway is crucial to extending this approach to new superlattice materials. The growth sequence observed for the $[TiSe_2]_n[NbSe_2]_n$ superlattices discussed in this paper is far from equilibrium as we kinetically trap the desired superlattice products. The diffraction data presented suggests that the reaction mechanism has an initial interdiffusion of the elements along the interfaces followed by interfacial nucleation of the binary components. These crystals grow in an oriented manner due to the asymmetric nature of the initial reactant. Near 500 °C, Ostwald ripening of the grains leads to a more oriented material, since grains misoriented relative to the initial layering must be smaller than those which grow along the layers. Annealing at higher temperatures leads to the mixing of the metals and the destruction of the superlattice. This new synthetic approach to crystalline superlattices results in the ability to rationally design an initial reactant which, upon controlled reaction, will result in a new compound with desired composition and superlattice structure.

Acknowledgment. This work was supported by the Office of Naval Research (N0014-93-1-0205). Additional support by the National Science Foundation (DMR-9308854 and DMR-9510562) is gratefully acknowledged.

JA9617653

(13) Foner, S.; McNiff, E. J. *J. Phys. Lett.* **1973**, *43A*, 429.